Comonomer Length Influence on the Structure and Mechanical Response of Metallocenic Polypropylenic Materials

Humberto Palza,* Juan M. López-Majada, Raúl Quijada, José M. Pereña, Rosario Benavente, Ernesto Pérez, María L. Cerrada*

The structure and properties have been comprehensively studied for metallocene copolymers of propylene-1-hexene (CiPH) and propylene-1-octadecene (CiPOD). The comonomer content constitutes the most important factor affecting both structure and properties in these CiPH and CiPOD copolymers, although the length of the comonomer is also very important. Thus, a considerable decrease in crystallinity and an easier obtainment of mesomorphic-like ordered entities are observed in the two kinds of copolymers as comonomer content increases. The variations in crystalline structure significantly influence the viscoelastic and mechanical behaviors of these CiPH and CiPOD copolymers. Consequently, the location and intensity of the different relaxation mechanisms as well as stiffness parameters (storage, Young's moduli, and microhardness) and deformation mechanism are strongly dependent upon composition.

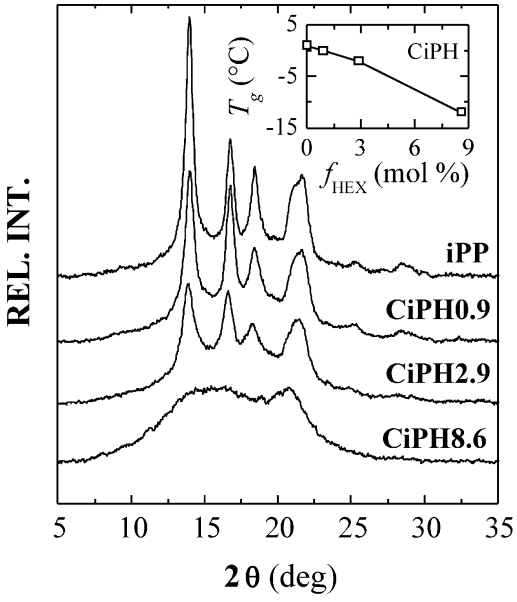

Introduction

Polyolefins are one of the most important plastics at industrial level because of their great production and constant growth in the last few years.[1,2] The synthesis of these polymers, specially polyethylenes and poly(propylene)s, underwent an important advance with the development of the Ziegler-Natta catalysts that together with new industrial processes allowed synthesizing a whole class of novel materials as, for example, polyethylenes with different microstructures (HDPE, LLDPE, etc.), poly(propylene) with controlled tacticities, new copolymers, etc.[2,3] In spite of the great advantage of using these Ziegler-Natta

H. Palza, R. Quijada
Departamento de Ingeniería Química, Facultad de Ciencias Físicas y Matemáticas, Universidad de Chile, Casilla 2777, Chile
Centro para la Investigación Multidisciplinaria Avanzada en Ciencias de los Materiales (CIMAT). Santiago, Chile
E-mail: hpalza@ing.uchile.cl
J. M. López-Majada, J. M. Pereña, R. Benavente, E. Pérez, M. L. Cerrada
Instituto de Ciencia y Tecnología de Polímeros (CSIC), Juan de la Cierva 3, 28006-Madrid, Spain
E-mail: mlcerrada@ictp.csic.es

catalytic systems, they present some problems derived from their multi-site characteristics, like broad molecular weight distribution (polydispersity always higher than 4) and heterogeneous interchain incorporation of comonomer in the case of copolymers, especially with large olefins.[4] Consequently, an inverse relationship between the comonomer content and copolymer molecular weight is obtained, which is explained by kinetic reasons and implies a broad distribution of comonomer content in the copolymer.[5] This characteristic of the Ziegler-Natta systems makes the detailed study of the effect of comonomer incorporation on the final properties of the polymer difficult. The only reliable possibility consists of fractionating the polymer and, subsequently, to study the properties of the different fractions. However, this method is rather expensive and a great amount of polymer is necessary, making a complete characterization difficult.

On the other hand, the discovery of cocatalysts like methylaluminoxane (MAO) was an important step for the development of highly activated metallocenic catalysts more than 20 years ago.[6,7] The most important characteristic of metallocenes is their single-site behavior, that allows synthesizing polyolefins with narrow molecular weight distribution (polydispersities near 2) and truly random copolymers with uniform intermolecular distribution of the comonomer content along the polymer, the low polydispersity being maintained.[5] In this way, the copolymers synthesized with metallocene catalysts are model-like materials to learn the effect of the comonomer content, or specifically the polymer microstructure, on the final properties of the material.

Many publications have reported studies on the influence of incorporating large olefins to the main chain of polyethylene.[8–12] The insertion of these comonomers changes the morphology of the polymer, specially the density and crystallinity, and the more important characteristic is that these variations depend on comonomer incorporation.[9,10,13] Therefore, these polymers can be classified within those labeled as tailor-made.

Comparable morphological alterations are found in isotactic propylene copolymers with 1-olefins, although the number of articles devoted to them is much lower.[14–16] An interesting finding is that a crystal structure neither resembles those of the well-known α, β, and γ phases of isotactic poly(propylene) (iPP) nor that of isotactic poly-1-hexene has been uncovered in copolymers of propylene-1-hexene (CiPH) with relatively high molar contents in 1-hexene (>10%), crystallized at moderate rates and annealed at room temperature.[17–19] On the other hand, specimens of low molecular weight CiPH copolymers with relatively low 1-hexene molar fractions (up to a 5 mol-%), prepared by a fast cooling from the molten state,[20] show a much easier formation of mesomorphic structures similar to those observed in either effective-quenched or stretched iPP.[21,22]

Moreover, the effect of comonomer size on the final properties is expected to be more dramatic in the case of propylene copolymers, although contradictory results have been reported in the open literature. On one hand, Van Reenen et al.[23] found that the type of comonomer (between 4 and 16 carbons within the lateral chains) does not influence the melting temperature, T_m, in these propylene copolymers and, on the other hand, Lovisi et al.[14] showed differences in T_m and in others properties (e.g., elastic modulus, density, etc.) for propylene with 1-hexene or 1-octene copolymers, depending on the type of the comonomer. They concluded that changes are more important in those copolymers with 1-octene as a comonomeric unit. Some differences with the length of the comonomer incorporated were also reported for syndiotactic propylene/α-olefins copolymers,[24] mainly in the amorphous regions and, accordingly, in the location of the glass transition temperature, T_g.

The main objective of this work is to analyze in detail the effect of the incorporation of 1-hexene and 1-octadecene in the structure and final properties of CiPH and propylene-1-octadecene (CiPOD) copolymers synthesized by an isospecific metallocene catalyst and processed at high cooling rates commonly used at the industrial final uses. The structural and thermal characterization has been carried out by wide-angle X-ray diffraction (WAXD) experiments, density measurements, and calorimetric analyses, whereas the evaluation of the viscoelastic behavior has been performed by dynamic-mechanical thermal analysis and the mechanical response, using uniaxial tensile stress–strain and microhardness measurements.

Experimental Part

Copolymerization of propylene with 1-hexene or 1-octadecene was performed as described elsewhere[15] with toluene as a solvent in a Slurry system in 1 L Buchi glass reactor, using the rac-$Me_2Si(2\text{-}Me\text{-}Ind)_2ZrCl_2$/MAO catalytic system. The results about either the comonomer or the stereo-defect contents in the different samples analyzed, determined by ^{13}C NMR spectroscopy, are shown in Table 1. The comonomer content was evaluated from these spectra using a known method[25] based on triads distribution ranging from 33.7 to 35.7 ppm and from 33.7 to 36 ppm for 1-hexene and 1-octadecene, respectively. On the other hand, the defects of stereo-regularity were estimated from resonances in the region of the methyl carbon atoms.[26] This avoids unwanted contributions from possible differences among nuclear Overhauser effects and relaxation times.[27] All these samples were fully regio-regular and then, no or negligible amounts of regio-defects were, indeed, detected in their ^{13}C NMR spectra. The different copolymers were labeled as CiPH and CiPOD for 1-hexene and 1-octadecene comonomer units, respectively, followed by a number that specifies their comonomer molar fractions.

The molecular weights were determined by gel permeation chromatography in a Waters 150 CV-plus system equipped with

Table 1. Characterization of the different propylene copolymers.

sample	Type of comonomer	Comonomer content mol-%	Comonomer content wt.-%	*mmmm* content %	*mmmr* content %	Total defects %	$\overline{M}_w$ kg · mol^{-1}	Density g · cm^{-3}	$f_c^{density}$	f_c^{WAXD}
iPP	–	0.0	0.0	95.0	2.2	1.1	224	0.905	0.62	0.60
CiPH0.9	1-hexene	0.9	1.8	94.7	1.8	1.8	215	0.899	0.55	0.52
CiPH2.9	1-hexene	2.9	5.6	95.0	1.2	3.5	174	0.893	0.47	0.42
CiPH8.6	1-hexene	8.6	15.8	96.1	1.0	9.1	183	0.882	0.33	0.25
CiPOD1.0	1-octadecene	1.0	5.7	94.2	2.0	2.0	189	0.895	0.50	0.52
CiPOD2.3	1-octadecene	2.3	12.4	95.6	1.0	2.8	230	0.890	0.43	0.40
CiPOD7.6	1-octadecene	7.6	33.0	97.6	1.2	8.2	195	0.882	0.33	0.25

an optical differential refractometer (model 150 °C). A set of three columns of the Styragel HT type (HT3, HT4, and HT6) was used with 1,2,4-trichlorobenzene as a solvent. Standards of polystyrene and polyethylene with narrow molecular mass distribution were used for calibration.

Sheets of each polymer were prepared by compression molding between hot plates at a temperature about 30 °C above the melting point in a Collin press at a pressure of around 15 bar. The samples were quenched from the molten state to room temperature between water plates at the same pressure. The thickness of the different films ranged from 0.5 to 0.6 mm.

Density determinations were performed at 23 °C in a water–ethanol gradient column that was calibrated with glass floats. The degree of crystallinity was calculated from the following equation:

$$f_c^{density} = \left[\frac{\rho_c}{\rho}\right]\left[\frac{\rho - \rho_a}{\rho_c - \rho_a}\right] \quad (1)$$

where ρ is the experimental density and the values of $\rho_a = 0.854$ g · cm^{-3} and $\rho_c = 0.936$ g · cm^{-3} are used for the amorphous and crystalline phase densities, respectively.[28]

Wide-angle X-ray diffraction patterns were recorded in the reflection mode at room temperature by using a Philips diffractometer with a Geiger counter, connected to a computer. Ni-filtered CuKα radiation was used. The diffraction scans were collected over a period of 20 min in the range of 2θ values from 3° to 43°. The goniometer was calibrated with the silicon standard. In general, the WAXD degree of crystallinity, f_c^{WAXD}, was determined from the X-ray diffractograms after subtraction of the amorphous profile.[29]

Calorimetric analyses were carried out in a Perkin Elmer DSC7 calorimeter connected to a cooling system and calibrated with different standards. The sample weights ranged from 6 to 9 mg and the heating rate used was 20 °C · min^{-1}. For crystallinity determinations, a value of 209 J · g^{-1} has been taken as the enthalpy of fusion of a perfect crystalline material.[30]

Dynamic mechanical relaxations were measured with a Polymer Laboratories MK II Dynamics Mechanical Thermal Analyzer, working in a tensile mode. The storage modulus, E', loss modulus, E'', and the loss tangent, tan δ, of each sample were obtained as function of temperature over the range from −150 to 150 °C at fixed frequencies of 1, 3, 10, and 30 Hz, and at a heating rate of 1.5 °C · min^{-1}. Strips of 2.2 mm wide and 15 mm length were cut from the molded sheets.

Stress–strain measurements were performed using an Instron dynamometer equipped with a load cell and an integrated digital display that provided force determinations. Dumbbell samples with an effective length of 15 mm and a width of 1.9 mm were cut from the compression-molded sheets. These specimens were then stretched at a strain rate of 10 mm · min^{-1} at 23 °C, and Young's modulus (E), yield stress (σ_y), and strain (ε_y) were determined. The Young's modulus was measured from the slope of the curve at very small deformations (the initial linear part of the curve). On the other hand, the yield stress and strain values were usually calculated from the maximum on the stress–strain curves obtained. If a maximum was not observed, the yield point was estimated by the tangent method. The values reported for Young's modulus, yield stress, and strain are averages from, at least, three different specimens of each sample.

The microhardness (MH) measurements were performed with a Vickers indentor. The MH values were estimated from the following expression:[31]

$$MH = 2\sin 68^\circ\left(\frac{P}{d^2}\right) \quad (2)$$

where P is the contact load (N) and d the length of the diagonal of the indentation surface (mm). All of the measurements were carried out with a load of 0.981 N and a contact time of 25 s at room temperature.

Results and Discussion

Structural and Thermal Properties

Table 1 shows the main characteristics of the different propylene copolymers synthesized with either 1-hexene or 1-octadecene comonomeric units. The tacticity was measured based on the *mmmm* pentad at 21.7 ppm

whereas the total amount of defects was calculated adding to the comonomer molar composition the half fraction of *mmmr* pentads, associated with the peak at 21.4 ppm. In this way, the total stereo-defect content can be determined independently of their structures,[27] since any stereo-defect sequence will have only two of these sequences. It is noteworthy that the values of the molecular weight and the *mmmm* and *mmmr* pentads are similar for all of these copolymers; these variables will not be, therefore, relevant for explanation of the different variations in the copolymer properties. In addition, it is also possible to observe the great effect of the comonomer content on density and, therefore, crystallinity ($f_c^{density}$) in these propylenic materials. Both structural parameters decrease as comonomer molar and, consequently, weight fractions increase. Density values in these CiPH correlate rather well with those reported in the literature for analogous copolymers.[19]

On the other hand, Figure 1 shows the WAXD profiles at room temperature for the different CiPOD copolymers and that found in the iPP homopolymer for comparison reasons. It can be observed that the profiles of the neat iPP and CiPOD1.0 and CiPOD2.3 copolymers exhibit the five main diffractions [(110), (040), (130), (111), and (130, 041) planes] characteristic of the α monoclinic iPP crystalline modification.[32,33] The intensity of the different reflections decreases and, consequently, crystallinity becomes smaller as the content of comonomer increases. Moreover, a broadening of diffractions and a shift of their location to lower angles are also evident. It is noticeable that no evidence of the γ modification is observed, most probably because of the high cooling rate used during processing of these copolymers.

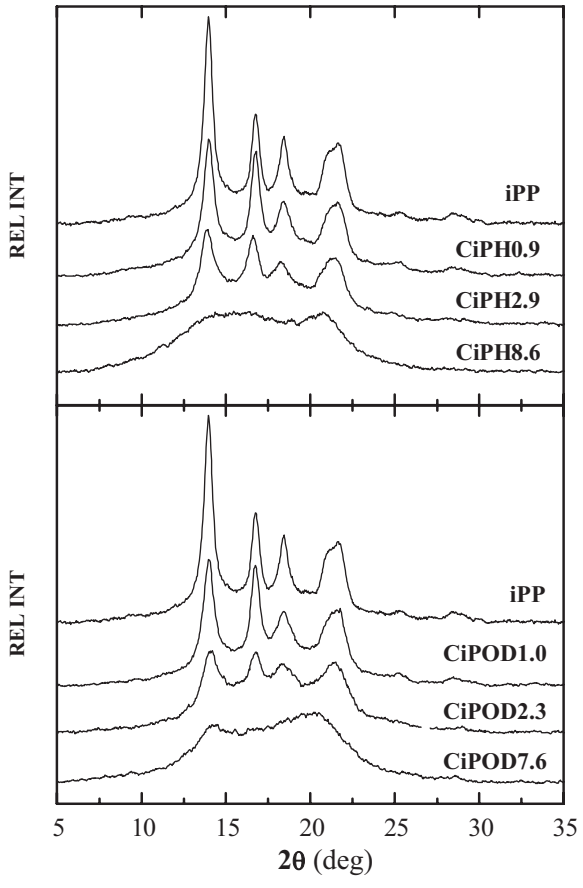

Figure 1. X-ray diffraction patterns, at room temperature, for iPP, CiPH, and CiPOD copolymers (top and bottom plots, respectively).

The CiPOD7.6 profile is, however, very analogous to that exhibited by the mesomorphic modification typical in Ziegler-Natta iPP homopolymers at extremely high cooling rates,[21,34] with two broad maxima at diffraction angles of around 14° and 21°. This profile is, evidently, somewhat different to that found for iPP homopolymer[35] due to the fact that now in this CiPOD7.6 sample, with a 33 wt.-% comonomer content, the non-crystalline profile is expected to have an important contribution at around 19°–20°, arising from the comonomer.

This mesomorphic profile is also observed in sample CiPH8.6, in agreement with features found in some other similar CiPH copolymers.[20,36] Moreover, the stretching of the γ polymorph in metallocene iPP also leads to the obtaining of this mesomorphic form.[37]

The degree of crystallinity deduced from the diffractograms, f_c^{WAXD}, is shown in the last column of Table 1. The results are very similar to those obtained from the density measurements.

Figure 2 shows the DSC curves related to the first melting process for the different samples. T_m values are significantly shifted to lower temperatures as comonomer content is increased (see results in Table 2). The same decreasing trend is found for crystallization temperatures. This shift of thermal transitions was explained many years ago by Flory[38] taking into account thermodynamic considerations. In particular, the change of the equilibrium melting point was described to follow the next equation:

$$\frac{1}{T} - \frac{1}{T_m^0} = -\frac{R}{\Delta H_u} \ln(X_A) \quad (3)$$

where ΔH_u is the enthalpy of fusion per repeating units of homopolymer, T_m^0 the melting temperature of the pure parent homopolymer, R the gas constant, and X_A is the fractions of propylene units in the molten copolymer. This equation is based on the exclusion model, where the comonomer acts like defect and is excluded from crystal lattice. This assumption is valid in the copolymers with 1-octadecene, because of the considerable length of this comonomer. The non-inclusion of comonomer within crystallites reduces the length of the main chain able to crystallize and, consequently, crystallinity as well as

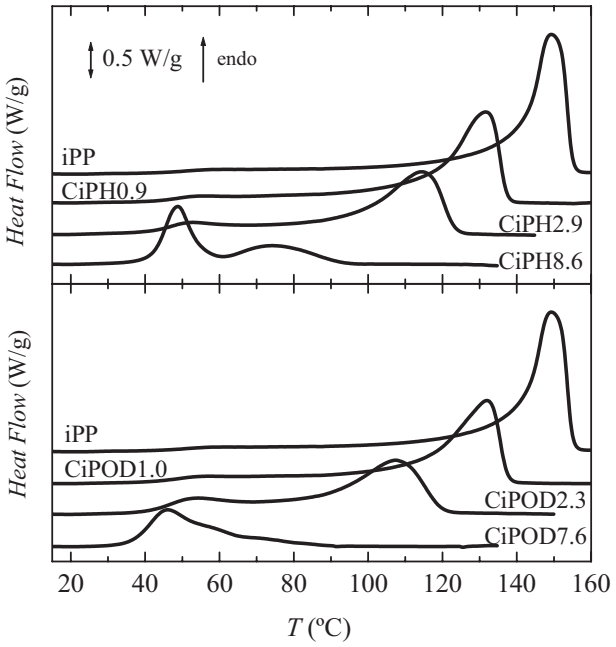

Figure 2. DSC first melting curves performed at 20 °C · min^{-1} in the iPP homopolymer and in the CiPH (top plot) and CiPOD (bottom plot) copolymers.

crystal thickness. Moreover, crystal lattice is substantially distorted, as aforementioned. However, it has been reported that 1-hexene is partially included in the crystalline structure,[19] so that Equation (3) may not be valid for the 1-hexene copolymers.

Additionally, a clear annealing peak is exhibited in the different samples. There is an important fraction of the sample that has crystallized into rather small and imperfect crystallites because of the fast cooling applied during processing. Therefore, these crystalline entities are able to melt and recrystallize during the stay of samples at room temperature prior to their analysis and, consequently, the initial smaller crystallites are slightly enlarged leading to the appearance of that peak located at 40–50 °C. This feature is important at a practical level because of its influence on the mechanical response.[13] Moreover, in the copolymers with the highest comonomer contents, there is a rather prominent peak centered at around 45–50 °C. Our interpretation is now that this endotherm might also correspond, at least partially, with the disappearance of the mesomorphic entities and/or its conversion into the regular monoclinic crystals, as it happens in iPP homopolymer.[39,40] Real-time variable temperature experiments employing synchrotron radiation are being planned in order to analyze this aspect.

Table 2. DSC values for the different thermal transitions existing in the first melting process: Glass transition, T_g, and melting, T_m, temperatures. Crystallization temperature during cooling, T_c, is also reported. The DSC crystallinity, f_c^{DSC}, is evaluated in the first melting and has been normalized for the actual weight amount of iPP component.

Sample	T_g	T_m	f_c^{DSC}	T_c
	°C	°C		°C
iPP	1	149	0.47	104
CiPH0.9	0	132	0.43	87
CiPH2.9	−2	114	0.39	68
CiPH8.6	−12	74	0.25	5
CiPOD1.0	−11	132	0.41	81
CiPOD2.3	−28	108	0.38	59
CiPOD7.6	−33	66[a)]	0.22	4

[a)] T_m value for the second melting process after in situ crystallization in the calorimeter.

On the other hand, the melting enthalpy is also significantly reduced when comonomer content increases in the copolymer. The introduction of more comonomeric units hinders the chain regularity needed for the crystallization process. Consequently, the crystallinity degree of these copolymers, estimated from the melting enthalpy normalized to the actual amount of crystallizable component, is lowered as the comonomer content increases, as listed in Table 2. These values prove that the decrease observed as comonomer content increases of parameters associated with the crystalline regions (melting and crystallization temperatures as well as normalized f_c^{DSC}), is slightly more significant for the CiPOD copolymers than for the CiPH ones.

Another very interesting feature from the DSC heating curves is the behavior of the glass transition. A significant variation of T_g is observed with both the comonomer content and the type of comonomer, as depicted in Figure 3 for the initial melting. It seems clear that the depression of the glass transition is deeper as either the composition or the length of the comonomer increases in the copolymer. Thus, a reduction of around 34 °C is observed in the case of the copolymer CiPOD7.6, although it has to be considered that this sample incorporates a 33% by weight of 1-octadecene comonomer. Accordingly, mobility within the amorphous regions is considerably much higher as length in the comonomeric unit is increased.

Dynamic-Mechanical Response

Figure 4 and 5 represent the DMTA curves for poly(propylene) and their CiPH and CiPOD copolymers as a function of temperature. Several relaxations are observed and the numeric values based on tan δ at 3 Hz are reported in Table 3. The relaxation at the highest temperature, named as α, is related to motions within the polymer crystalline phase, especially with defect diffusion.[41] As

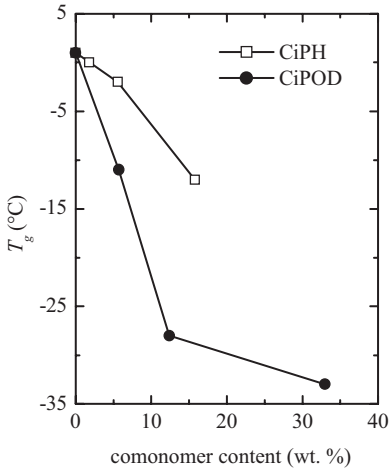

Figure 3. Dependence of glass transition temperature, T_g, determined from the first melting process performed at 20 °C · min^{-1}, on weight comonomer content for the different CiPH and CiPOD copolymers.

the comonomer content increases, the location of the α-relaxation is shifted to lower temperatures, as seen from the E' and E'' plots, because of the reduction in crystallinity and crystal size, as previously discussed. It has been reported that changes in the amorphous phase can also explain the behavior of this relaxation in copolymers due to the drifts in properties of the interphase,[16] helping to relax the diffusion of ending defects in that region.[41]

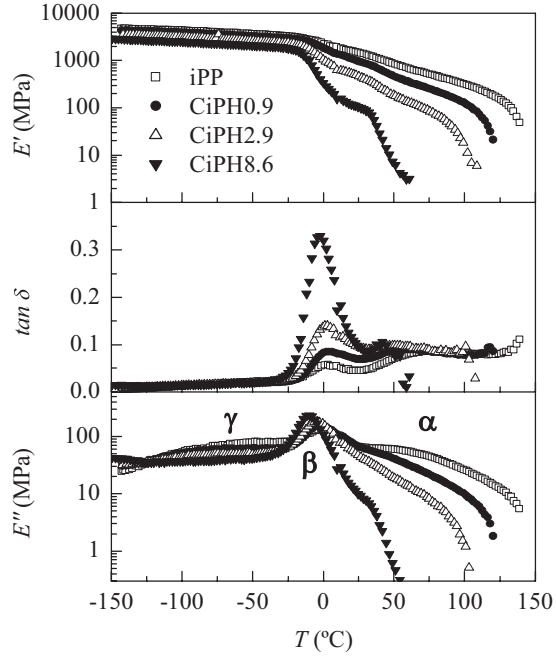

Figure 4. Variation of the storage modulus (E'), tan δ, and loss modulus (E'') with temperature at 3 Hz for iPP and the CiPH copolymers.

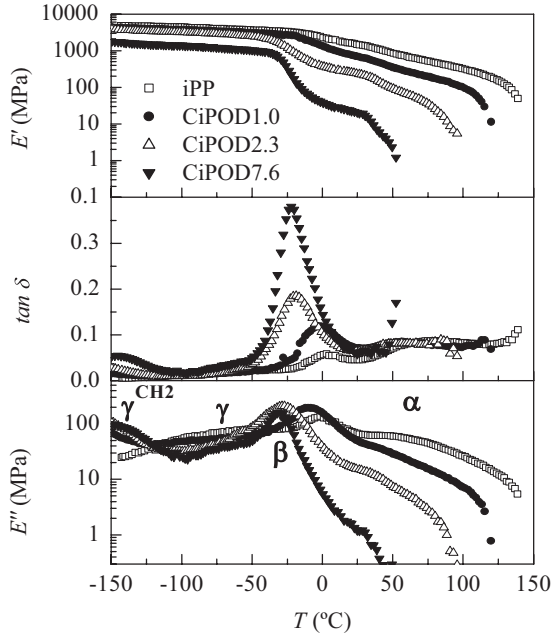

Figure 5. Variation of the storage modulus (E'), tan δ, and loss modulus (E'') with temperature at 3 Hz for iPP and the CiPOD copolymers.

The relaxation placed at around 0 °C is ascribed to generalized motions of the long chain segments characteristic of the glass transition. The cooperative nature of this movement explains the great descent in E' found in this temperature range. Intensity of this transition in tan δ rises as the comonomer content does in the copolymer because of the increase in the amorphous fraction within the polymeric materials. Moreover, the location of the β-relaxation changes with composition, shifting down to lower temperatures as increasing comonomer content. In agreement with the T_g calorimetric values, the β-relaxation in CiPOD copolymers shows a more significant decrease than in the CiPH ones, this fact being associated, on the one hand, with the higher flexibility of lateral chains with 16 carbons instead of those chains with 4 carbon links and, on the other hand, with the larger free volume caused by the longer comonomeric unit.[24]

Therefore, the incorporation of a small amount of 1-octadecene might be a good method to enhance the sometimes not sufficient impact resistance at low temperature of poly(propylene) homopolymer.[42] The area under the tan δ curve, from −150 to 30 °C, is consequently given in Table 3 because this value is a good parameter correlating rather well with the impact strength of the material.[43,44]

Other relaxation process, labeled as γ and ascribed to rotational motion of methyl groups from poly(propylene), is observed at temperatures slightly lower than that related to cooperative motions. It does actually appears as

Table 3. Location of main relaxation processes on tan δ basis at 3 Hz, and area under tan δ curves from −150 °C to 30 °C.

Sample	T_α	T_β	Area under tan δ curve (arbitrary units)
	°C	°C	
iPP	82	5	4.3
CiPH0.9	60	4	5.2
CiPH2.9	51	2	7
CiPH8.6	–	−3	12
CiPOD1.0	56	−1	7
CiPOD2.3	47	−19	10
CiPOD7.6	–	−22	16

a shoulder and not as a well-defined peak (see Figure 4 and 5). In addition to this γ mechanism, the CiPOD copolymers show an extra relaxation,[16,24] named as γ^{CH_2}, at around −150 °C. This new process seems to have the same molecular cause that the γ-relaxation [16,45,46] in polyethylene has, which requires, at least, three or more consecutive methylene units. Thus, the presence of this γ^{CH_2} relaxation is also dependent on the type of the comonomer, although this mechanism could be observed in the CiPH copolymers if the 1-hexene composition is high enough and, for instance, in CiPH8.6 copolymer is slightly noticeable.

Stress–strain and Microhardness Measurements

Figure 6 shows the results from stress–strain tests in both CiPH and CiPOD copolymers. Great changes are observed in the main mechanical parameters when the comonomer content varies. The most relevant variations are observed in the yielding point and in elastic modulus, as seen in Table 4. The former becomes diffuse and the latest is reduced as comonomer fraction increases, indicating the transition from the necking deformation process typically exhibited by thermoplastic polymers to a ductile and elastomeric-like mechanism.[10,13,16] The decrease in crystallinity and the subsequent increase in flexibility in the copolymers are responsible of changing the mechanism of deformation. The amorphous phase behaves as a viscoelastic liquid with a low stress resistance compared with that exhibited by the crystal phase. Therefore, as the crystallinity is reduced the content of amorphous regions is enlarged and, consequently, the stress resistance is lowered and the capability of being deformed is significantly enlarged.

The aforementioned higher mobility found in the amorphous regions of CiPOD copolymers again shows up and the mechanical parameters obtained from the stress-strain curves consequently change. Those related to

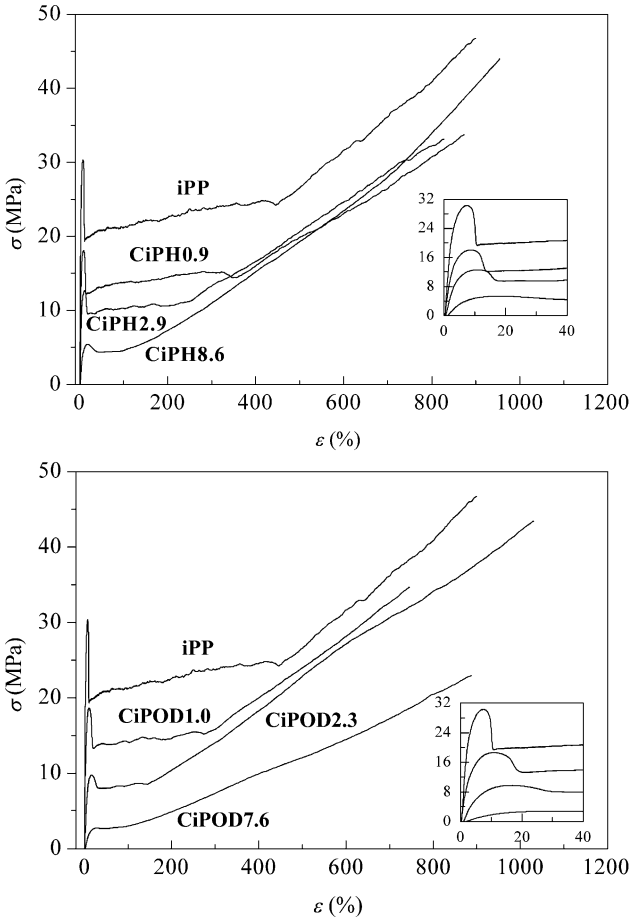

Figure 6. Stress–strain curves for the iPP, different CiPH, and CiPOD copolymers.

the stiffness, elastic modulus and magnitude, of yield stress are minimized, as seen in Figure 6 and Table 4, whereas deformation at yield and at break displays higher values as 1-octadecene is the comonomeric unit copolymerized.

The decrease in the elastic modulus and yield stress with increasing comonomer concentration and, therefore,

Table 4. Main mechanical parameters obtained from stress–strain measurements for the different propylene copolymers.

Sample	E	σ_Y	ε_Y
	MPa	MPa	%
iPP	1100	29	7
CiPH0.9	726	21	8
CiPH2.9	388	14	11
CiPH8.6	100	6	18
CiPOD1.0	555	20	11
CiPOD2.3	187	10	16
CiPOD7.6	20	3	27

lowering crystallinity here commented has also been found in some other ethylene or hexene copolymers[36,47] whereas a different response is observed for copolymers with 1-butene as a comonomeric unit, the Young's modulus being nearly constant with changing 1-butene composition[47].

Moreover, the effect of the comonomer type on mechanical response is also confirmed by microhardness, MH, values. The MH involves a complex combination of properties: elastic modulus, yield strength, strain hardening, and toughness. Figure 7 shows its dependence on the content and type of comonomer. It can be seen that CiPOD copolymers show lower values than CiPH ones at similar contents due to the softer nature of the former propylene-based materials.

A direct relationship is commonly found between the elastic modulus and MH and the following empirical equation has been proposed:[31]

$$\mathrm{MH} = aE^b \tag{4}$$

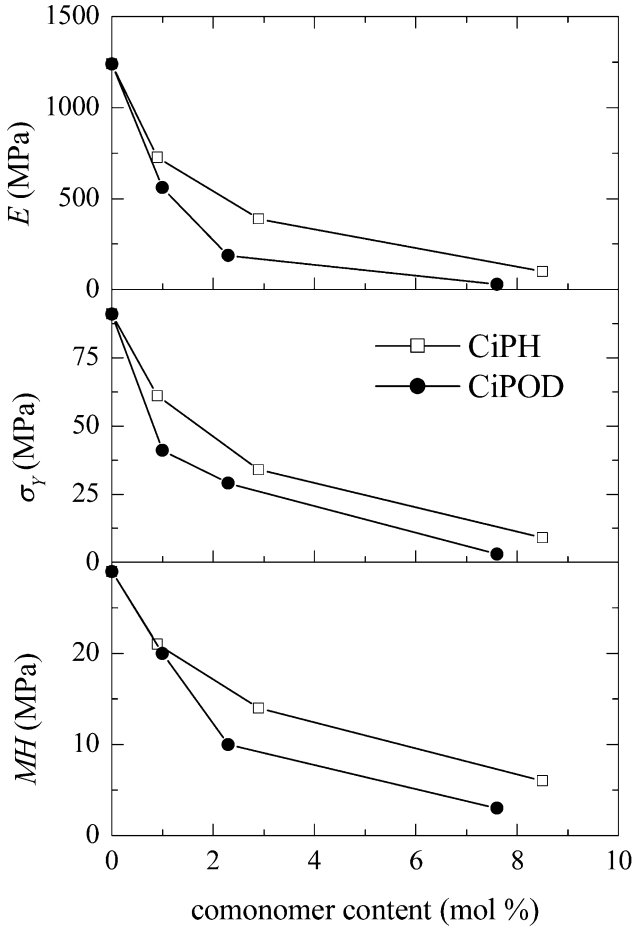

Figure 7. Effect of the comonomer content on the elastic modulus, yield stress, and microhardness for the different CiPH and CiPOD copolymers.

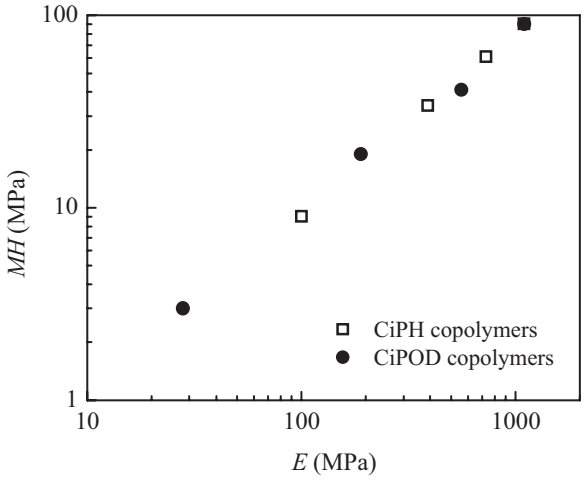

Figure 8. Relation between elastic modulus and microhardness based on Equation 4.

where MH is the microhardness value, E the elastic modulus, and a and b are constants. Consequently, if this relationship is accomplished, the variables that affect the elastic modulus are the same than those that influence the MH values. The constant b expresses a power dependence of the microhardness on the modulus, and is an indicator of the microhardness sensitivity toward the modulus of elasticity.[48] Figure 8 represents in a double logarithm scale the experimental values of MH and E for the CiPH and CiPOD copolymers under study and a good correlation is observed, Equation 4 being valid for these copolymers. The values for the constant b are 0.96 and 0.90 for CiPH and CiPOD, respectively. Then, the former copolymers seem to be slightly more sensitive with respect to changes in elastic moduli for the MH, indicating again the influence of the comonomer type.

Conclusion

A considerable decrease in crystallinity is observed with comonomer content in these CiPH and CiPOD copolymers. Moreover, the importance that comonomer type has in the structure has been described. The crystal lattice varies from a monoclinic cell at low molar fractions to mesomorphic-like ordered entities for the highest one. These variations in crystal structure significantly influence the viscoelastic and mechanical behavior of these copolymers.

Several relaxation processes take place, their location and intensity being strongly dependent upon composition. As comonomer content increases, the intensity of α-relaxation, ascribed to motions within crystalline regions, diminishes, and that related to the process associated with cooperative movements within amorphous phase (β-relaxation) increases. Moreover, a shift of their location to

lower temperatures is also observed for both processes. On the other hand, a relaxation related to internal motions within the comonomeric units (labeled as γ^{CH_2}) is seen in the range of very low temperatures if CH_2 content is high enough, i.e., in the CiPH8.6 and all of the CiPOD copolymers. This process is ascribed to the movements of methylenic segments within the comonomer and, consequently, is strongly dependent on the composition and length of incorporated units.

The cold-drawing deformation mechanism characteristic of iPP evolves to another rather homogeneous-like simply varying the composition when deformation takes place at room temperature. Rigidity strongly diminishes and impact strength — measured indirectly through integration of loss curves — increases with the comonomer content, these changes being more significant in the CiPOD copolymers.

Acknowledgements: The authors are grateful for the financial supports of *Ministerio de Educación y Ciencia* (projects MAT2005-00228 and MAT2007-65519-C02-01) and of CONICYT (project FONDAP 11980002). We also thank Dr. *G. Galland* her help in the ^{13}C-NMR analysis performed for different specimens.

Received: June 2, 2008; Revised: August 13, 2008; Accepted: August 13, 2008; DOI: 10.1002/macp.200800294

Keywords: amorphous; isotactic poly(propylene); metallocene catalyst; propylene-1-hexene copolymers; propylene-1-octadecene copolymers

[1] D. Foxley, *Chem. Ind.* **1998**, *9*, 305.
[2] P. Galli, G. Vecellio, *J. Polym. Sci., Part A: Polym. Chem.* **2003**, *42*, 396.
[3] J. Huang, G. L. Rempel, *Prog. Polym. Sci.* **1995**, *20*, 459.
[4] J. Suhm, M. J. Schneider, R. Mülhaupt, *J. Mol. Catal. A:Chem.* **1998**, *128*, 215.
[5] R. Mülhaupt, *Macromol. Chem. Phys.* **2003**, *204*, 289.
[6] W. Kaminsky, *Adv. Catal.* **2001**, *47*, 89.
[7] W. Kaminsky, A. Laban, *Appl. Catal. A:Gen.* **2001**, *222*, 47.
[8] S. Bensason, J. Minick, A. Moet, S. Chum, A. Hiltner, E. Baer, *J. Polym. Sci., Part B: Polym. Phys.* **1996**, *34*, 1301.
[9] A. Alizadeh, L. Richardson, J. Xu, S. McCartney, H. Marand, Y. W. Cheung, S. Chum, *Macromolecules* **1999**, *32*, 6221.
[10] M. L. Cerrada, R. Benavente, B. Peña, E. Pérez, *Polymer* **2000**, *41*, 5957.
[11] M. L. Cerrada, R. Benavente, E. Pérez, *J. Mater. Res.* **2001**, *16*, 1103.
[12] R. Benavente, E. Pérez, M. Yazdani-Pedram, R. Quijada, *Polymer* **2002**, *43*, 6821.
[13] R. Benavente, E. Pérez, R. Quijada, *J. Polym. Sci., Part B: Polym. Phys.* **2001**, *39*, 277.
[14] H. Lovisi, M. I. Tavares, N. M. da Silva, S. M. C. de Menezes, L. C. de Santa Maria, M. B. Coutinho, *Polymer* **2001**, *42*, 9791.
[15] R. Quijada, J. L. Guevara, G. B. Galland, F. M. Rabagliati, J. M. López-Majada, *Polymer* **2005**, *46*, 1547.
[16] H. Palza, J. M. López-Majada, R. Quijada, R. Benavente, E. Pérez, M. L. Cerrada, *Macromol. Chem. Phys.* **2005**, *206*, 1221.
[17] B. Poon, M. Rogunova, A. Hiltner, E. Baer, S. P. Chum, A. Galeski, E. Piorkowska, *Macromolecules* **2005**, *38*, 1232.
[18] B. Lotz, J. Ruan, A. Thierry, G. C. Alfonso, A. Hiltner, E. Baer, E. Piorkowska, A. Galeski, *Macromolecules* **2006**, *39*, 5777.
[19] C. De Rosa, S. Dello Iacono, F. Auriemma, E. Ciaccia, L. Resconi, *Macromolecules* **2006**, *39*, 6098.
[20] J. M. López-Majada, H. Palza, J. L. Guevara, R. Quijada, M. C. Martínez, R. Benavente, J. M. Pereña, E. Pérez, M. L. Cerrada, *J. Polym. Sci., Part B: Polym. Phys.* **2006**, *44*, 1253.
[21] R. Androsch, B. Wunderlich, *Macromolecules* **2001**, *34*, 5950.
[22] R. F. Saraf, *Polymer* **1994**, *35*, 1359.
[23] A. J. Van Reenen, R. Brull, U. M. Wahner, H. G. Raubenheimer, R. D. Sanderson, H. Pash, *J. Polym. Sci., Part A: Polym. Chem.* **2000**, *38*, 4110.
[24] J. Arranz-Andrés, J. L. Guevara, T. Velilla, R. Quijada, R. Benavente, E. Pérez, M. L. Cerrada, *Polymer* **2005**, *46*, 12287.
[25] M. Kakugo, Y. Naito, K. Mizunama, T. Miyakate, *Macromolecules* **1982**, *15*, 1150.
[26] L. Resconi, A. Fait, F. Piemontesi, M. Colonnesi, H. Rychlicki, R. Zeigler, *Macromolecules* **1995**, *28*, 6667.
[27] R. G. Alamo, J. A. Blanco, P. K. Agarwal, J. C. Randall, *Macromolecules* **2003**, *36*, 1559.
[28] J. Brandrup, E. H. Immergut, E. A. Grulke, "*Polymer Handbook*", John Wiley, New York **1999**.
[29] S. Mansel, E. Pérez, R. Benavente, J. M. Pereña, A. Bello, W. Roll, R. Kirsten, S. Beck, H.-H. Brintzinger, *Macromol. Chem. Phys.* **1999**, *200*, 1292.
[30] B. Wunderlich, "*Macromolecular Physics*", Vol. 3, Academic Press, New York **1980**, p. 42.
[31] F. J. Baltá Calleja, *Adv. Polym. Sci.* **1985**, *66*, 117.
[32] A. Turner-Jones, *Polymer* **1971**, *12*, 487.
[33] J. Arranz-Andrés, R. Benavente, E. Pérez, M. L. Cerrada, *Polym. J.* **2003**, *35*, 766.
[34] L. E. Alexander, "*X-ray Diffraction Methods in Polymer Science*", Ed. Wiley-Interscience, New York 1969.
[35] T. Konishi, K. Nishida, T. Kanaya, K. Kaji, *Macromolecules* **2005**, *38*, 8749.
[36] J. Arranz-Andrés, I. Suárez, B. Peña, R. Benavente, E. Pérez, M. L. Cerrada, *Macromol. Chem. Phys.* **2007**, *208*, 1510.
[37] C. De Rosa, F. Auriemma, A. Di Capua, L. Resconi, S. Guidotti, I. Camurati, I. E. Nifant'ev, I. P. Laishevtsev, *J. Am. Chem. Soc.* **2004**, *126*, 17040.
[38] P. J. Flory, *Trans. Faraday Soc.* **1955**, *51*, 848.
[39] R. F. Saraf, R. S. Porter, *Polym. Eng. Sci.* **1988**, *28*, 842.
[40] S. Osawa, R. S. Porter, *Polymer* **1994**, *35*, 545.
[41] C. Jourdan, J. Y. Cavaille, J. Perez, *J. Polym. Sci., Part B: Polym. Phys.* **1989**, *27*, 2361.
[42] C.-F. Ou, *Eur. Polym. J.* **2002**, *38*, 467.
[43] O. Prieto, J. M. Pereña, R. Benavente, E. Pérez, M. L. Cerrada, *J. Polym. Sci., Part B: Polym. Phys.* **2003**, *41*, 1878.
[44] F. Ramsteiner, *Polymer* **1979**, *20*, 839.
[45] R. H. Boyd, R. S. Breitling, *Macromolecules* **1974**, *7*, 855.
[46] N. J. Heaton, R. Benavente, E. Pérez, A. Bello, J. M. Pereña, *Polymer* **1996**, *37*, 3791.
[47] C. De Rosa, F. Auriemma, O. Ruiz de Ballesteros, L. Resconi, I. Camurati, *Chem. Mater.* **2007**, *19*, 5122.
[48] G. Zamfirova, V. Lorenzo, R. Benavente, J. M. Pereña, *J. Appl. Polym. Sci.* **2003**, *88*, 1794.